

## Accepted Article

**Title:** Expanding Anti-Stokes Shifting in Triplet-triplet Annihilation Upconversion for In Vivo Anticancer Prodrug Activation

**Authors:** huang ling, yang zhao, he zhang, kai huang, jingyi yang, and Gang Han

This manuscript has been accepted after peer review and appears as an Accepted Article online prior to editing, proofing, and formal publication of the final Version of Record (VoR). This work is currently citable by using the Digital Object Identifier (DOI) given below. The VoR will be published online in Early View as soon as possible and may be different to this Accepted Article as a result of editing. Readers should obtain the VoR from the journal website shown below when it is published to ensure accuracy of information. The authors are responsible for the content of this Accepted Article.

**To be cited as:** *Angew. Chem. Int. Ed.* 10.1002/anie.201704430  
*Angew. Chem.* 10.1002/ange.201704430

**Link to VoR:** <http://dx.doi.org/10.1002/anie.201704430>  
<http://dx.doi.org/10.1002/ange.201704430>

# Expanding Anti-Stokes Shifting in Triplet–Triplet Annihilation Upconversion for In Vivo Anticancer-Prodrug Activation

Ling Huang<sup>[a]</sup> ‡, Yang Zhao<sup>[a]</sup> ‡, He Zhang<sup>[a]</sup>, Kai Huang<sup>[a]</sup>, Jingyi Yang<sup>[a]</sup>, and Gang Han<sup>[a]\*</sup>

**Abstract:** A strategy to expand anti-Stokes shifting from the far-red to deep-blue region in metal-free triplet–triplet annihilation upconversion (TTA-UC) is presented and its utility in the *in vivo* titration of the photorelease of an anticancer prodrug is demonstrated. This new TTA system has robust brightness and the longest anti-Stokes shift of any reported TTA system. TTA core-shell-structured prodrug delivery capsules that benefit from these properties are developed; they can operate with low-power-density far-red light-emitting diode (LED) light. These capsules contain mesoporous silica nanoparticles preloaded with TTA molecules as the core and amphiphilic polymers encapsulating anticancer prodrug molecules as the shell. When stimulated by far-red light, the intense TTA upconversion blue emission in the system activates the anticancer prodrug molecules and shows effective tumor growth inhibition *in vivo*. This work paves the way for the design of new organic TTA upconversion with regard to *in vivo* photocontrollable drug release and other biophotonic applications.

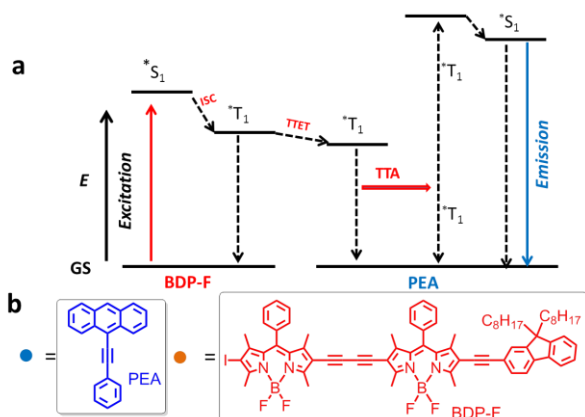
In recent years, the development of stimulus-responsive prodrug release and delivery systems has been of great interest to the fields of chemistry and biology. These systems effectively improve the therapeutic efficacy of drug release in malignant sites with minimal side-effects.<sup>[1]</sup> Compared to other drug-release strategies, light-induced prodrug activation is unique, with noninvasive operation and high spatiotemporal controllability.<sup>[2]</sup> In such a strategy, drug molecules are typically modified and protected with light-sensitive chromophores, such as coumarin, 2-nitrobenzyl, and 7-nitroindoline. However, these chromophores typically require short-wavelength deep-blue light (ca. 435 nm) or phototoxic ultraviolet (UV) light (ca. 365 nm) as the excitation light sources; these methods also suffer rather poor tissue penetration depth in their *in vivo* applications.<sup>[3]</sup>

To address this problem, long-wavelength light was recently utilized in the therapeutic window (600–900 nm) due to its minimal absorption by tissue and its deep-tissue penetration.<sup>[4]</sup> For example, lanthanide ion-doped inorganic upconversion nanoparticles (UCNPs) can convert tissue-penetrable long-wavelength light into high-energy short-wavelength photons to trigger small-molecule drug release.<sup>[3c,5]</sup> However, challenges

remain in regard to inorganic UCNPs. For instance, due to the intrinsic low absorption and emission cross-sections of the contained lanthanide ions, such UCNPs have quite low quantum yields that typically require relatively high-power-density laser excitation. The long-term *in vivo* toxicity and systematic clearance of inorganic lanthanide ions inside UCNPs are also unclear.<sup>[3d,6]</sup> These key limitations have led to the exploitation of a more biocompatible upconversion strategy, particularly with respect to the emerging organic-chromophore-based triplet–triplet annihilation upconversion (TTA-UC). In regard to TTA-UC, low-energy photons can be absorbed by a sensitizer chromophore and then transferred to an acceptor chromophore through a unique triplet–triplet energy-transfer process. Two excited acceptor molecules subsequently undergo a TTA annihilation process, to generate one high-energy short-wavelength photon (**Scheme 1a**). Compared to inorganic UCNPs, TTA-UC offers some advantages due to its intense absorption coefficient of sensitizers, high quantum yield and brightness, as well as the concomitant low-power-density excitation resource.<sup>[7]</sup> Therefore, TTA-UC-based materials are potentially suitable for applications as photocontrollable drug-delivery systems. Quite recently, green-to-blue TTA-UC nanomicelles were fabricated to trigger the uncaging of blue-light-sensitive coumarin-group-modified peptides, thus enabling better subsequent cell targeting.<sup>[8]</sup> However, *in vivo* drug photorelease and concomitant cancer treatment are formidable challenges, as the green excitation source lacks deep-tissue penetration depth and yields low quantum efficiency. Moreover, such TTA-UC remains insufficient to activate a large number of prodrug molecules for cancer treatment.<sup>[9]</sup> To address this problem, some deep-tissue-penetrable TTA systems that are excitable with longer wavelength light were proposed. For example, a TTA system containing meso-tetraphenyl-tetrabenzoporphine palladium PdTPBP (sensitizer) and perylene (emitter) can upconvert 635 nm laser light to 475 nm photons and was used for the photodissociation of ruthenium polypyridyl complexes from PEGylated liposomes in water.<sup>[9c,10a]</sup> However, the existing system has limitations to its *in vivo* applications due to its suboptimal efficiency and relatively high excitation power density (2.3 W cm<sup>-2</sup>), which is beyond the biosafety threshold.<sup>[10a]</sup> In addition, the anti-Stokes-shifted emission wavelength of 475 nm is not compatible with the typical deep blue/UV operation wavelengths for biologically used caging groups.<sup>[3]</sup> To this end, the development of a new TTA system with dramatically improved anti-Stokes shifting from far red to deep blue and robust brightness properties is highly desirable.

[a] L. Huang, Dr. Y. Zhao, H. Zhang, Dr. K. Huang, J. Yang, Prof. Dr. G Han  
Department of Biochemistry and Molecular Pharmacology  
University of Massachusetts Medical School  
Worcester, MA 01605, United States.  
E-mail: Gang.Han@umassmed.edu

‡ equal contribution



**Scheme 1.** a) A Jablonski diagram of the photophysical processes of the triplet photosensitizers and the TTA upconversion exemplified with BDP-F as the triplet photosensitizer and PEA as the emitter; b) molecular structure of BDP-F and PEA.

In this study, to achieve far red to deep blue TTA-UC, we designed a metal-free iodized BODIPY dimer (BDP-F) molecule to be used as a highly far-red-sensitive photosensitizer and 9-phenylacetylene anthracene (PEA) as a deep blue emitter (**Scheme 1b**). Compared to conventional BODIPY photosensitizers, such as 2,6-diiodo-BODIPY ( $\epsilon = 85\,000\text{ M}^{-1}\text{ cm}^{-1}$  at 525 nm, **Scheme S2**), due to its large  $\pi$  core, BDP-F presented broader and more intense absorption in the far-red region from 600–670 nm (peaking at 615 nm,  $\epsilon = 1.77 \times 10^5\text{ M}^{-1}\text{ cm}^{-1}$ ; **Figure 1a**). Meanwhile, BDP-F has an outstanding triplet-state lifetime ( $\tau_T = 243.6\text{ }\mu\text{s}$ ; **Figure S1**) that is essential for the TTA photosensitizers. To increase the anti-Stokes-shifted deep-blue emission, 9-phenylacetylene anthracene (PEA) was synthesized as a new emitter (**Scheme S1**). PEA presents excellent fluorescence quantum yield in the deep-blue region from 410–500 nm, peaking at 432 nm ( $\Phi_f = 87\%$ ; **Figure S2**), which makes it particularly suitable as the emitter.

We then further optimized the concentration ratio of BDP-F and PEA in the TTA-UC system. The best combination was 20  $\mu\text{M}$  of BDP-F and 200  $\mu\text{M}$  of PEA in degassed toluene solution (**Figure S3, S4**). At this optimal ratio, intense deep-blue emission in the range of 410–500 nm can be observed by the naked eye upon irradiation with 650-nm light (**Figure 1b**). This TTA-UC system showed a high relative upconversion quantum yield ( $\Phi_{\text{UC}} = 3.1\%$ ) when methyl blue was used as a reference.<sup>[7a, 10b, 10c]</sup> The TTA-UC also presented excellent upconversion brightness ( $\eta = \epsilon \times \Phi_{\text{UC}}$ , 1054 at 100  $\text{mW cm}^{-2}$  of 650-nm light). More importantly, to our knowledge, our TTA-UC system presents the longest anti-Stokes shift ( $\Delta\lambda = 0.96\text{ eV}$ ) of any reported TTA upconversion system (see **Table S1**). Further, the TTA upconversion intensity threshold ( $I_{\text{th}}$ ) was studied (**Figure S5**). Quadratic dependence of the upconversion emission was observed for low-energy incident power density excitation and a linear region observed at higher incident power densities in deaerated toluene. The transition threshold ( $I_{\text{th}}$ ) between the quadratic and the linear regime occurs near 19.6  $\text{mW cm}^{-2}$ , which is comparable to the value of reported TTA-UC systems.<sup>[11a]</sup> A power-dependence experiment provided evidence for TTA-UC in BDP-F and PEA system in deaerated toluene.<sup>[11b]</sup>

Because of these excellent photophysical properties, we sought to construct a TTA-UC drug-delivery system based on

our new TTA system. In particular, we designed a TTA upconversion core/shell structured nanocapsule (TTA-CS) in two steps (**Scheme S3**). In the first step, TTA-MSNs are formed by infusing a TTA-UC dye pair (20  $\mu\text{M}$  of BDP-F and 200  $\mu\text{M}$  of PEA) in methyl oleate oil into mesoporous channels of silica nanoparticles. In the second step, TTA-CS is further developed by adding a layer of the prodrug coumarin–chlorambucil (Cou-C, see **Figure 2**)<sup>[12]</sup> onto the TTA-MSNs that were made during the first step. After uncaging, the prodrug (Cou-C) is able to convert into hydrophilic chlorambucil, which can be released from the TTA-CS and then kill the tumor cells.

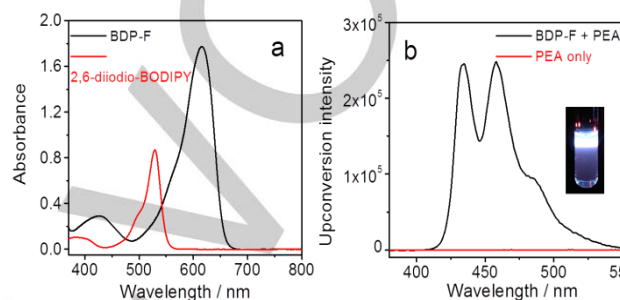


**Figure 1.** a) UV-vis absorption spectra of BDP-F and 2,6-diiodo-BODIPY (10  $\mu\text{M}$ ) in toluene at room temperature. b) The upconversion emission spectra of BDP-F (20  $\mu\text{M}$ ) and PEA (0.2 mM) in degassed toluene,  $\lambda_{\text{ex}} = 650\text{ nm}$  (100  $\text{mW cm}^{-2}$ ), inset shows such TTA-UC can be observed with the naked eye.

Firstly, we found that methyl oleate oil can efficiently prevent oxygen quenching of TTA-UC, as seen in **Figure S6a**. There was only 6% upconversion intensity reduction in air compared to in argon. In addition, the TTA-UC system of BDP-F and PEA in methyl oleate was quite stable; even after 20 days, the upconversion emission intensity was reduced by only 9.0% in air (**Figure S6b**). Subsequently, TTA-UC (20  $\mu\text{M}$  of BDP-F and 200  $\mu\text{M}$  of PEA) in methyl oleate oil was infused into mesoporous channels of silica nanoparticles to form TTA-MSNs. The TTA-MSNs were characterized by using transmission electron microscopy (TEM). As shown in **Figure S7**, the TEM image indicates that the TTA-MSNs consist of uniform spherical nanoparticles with a diameter of  $218 \pm 16\text{ nm}$ . The hydrodynamic diameter is  $259 \pm 12\text{ nm}$  as measured by dynamic light scattering (DLS) in deionized (DI) water. As shown in **Figure S8**, upon excitation with 650-nm light, the TTA-MSNs generated a deep, bright-blue upconversion emission that peaks at 430 nm. By using methyl blue as the reference, the upconversion quantum yield ( $\Phi_{\text{UC}}$ ) of TTA-MSNs in water was measured to be 2.0% (100  $\text{mW cm}^{-2}$ ) in air. The photostability of the TTA-MSNs was also investigated in air. No significant changes in the TTA-UC were observed when TTA-MSNs were continuously irradiated by using a 650-nm laser (100  $\text{mW cm}^{-2}$ ) for 30 min (**Figure S9**). This result suggests that the TTA-MSNs have excellent photostability.

Secondly, as shown in **Scheme S3**, a TTA-CS was prepared by adding a layer of the amphiphilic polymer F-127 encapsulated deep blue light sensitive hydrophobic prodrug coumarin–chlorambucil<sup>[12]</sup> onto the TTA-MSNs. In TTA-CS, chlorambucil was chosen because it is a potent and cost-effective small-molecule tumor inhibitor<sup>[9b, 12]</sup>. Moreover, the coumarin-based group possesses high photocleavage efficiency and a deep-blue absorption wavelength, the latter of which overlaps with the

emission spectrum of PEA (Figure S10).<sup>[4c]</sup> As seen in Figure S11a, the deep-blue upconversion emission of the resulting TTA-CS is less than that of the TTA-MSNs, which suggests that absorbs the 430 nm light was successfully encapsulated within the system. The core/shell nanocapsule was further characterized by using DLS. The hydrodynamic diameter of the TTA-CS ( $358 \pm 27$  nm) is larger than the diameter of the TTA-MSNs (Figure S11b), which suggests that the amphiphilic polymer F-127 encapsulated prodrug is the external shell in the system. The prodrug entrapment efficiency was calculated by a previously reported method to be 79% (see Supporting Information). The rate of release of prodrug from the TTA-CSs in the absence of 650-nm light is rather insignificant (ca. 4.4% after 24 h; Figure S12).

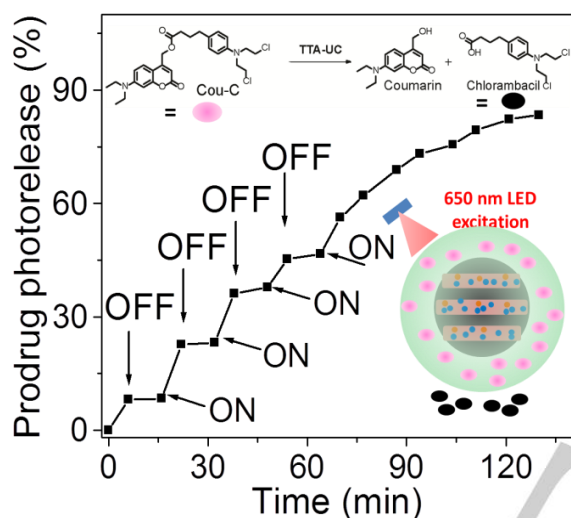


**Figure 2.** The TTA-upconversion regulated activation of Cou-C from TTA-CS with 650-nm-LED irradiation. "ON" and "OFF" indicate the initiation and termination of LED irradiation, respectively, and the working power density was  $100 \text{ mW cm}^{-2}$ . Top inset: the photoactivation reaction of Cou-C; bottom inset: schematic illustration of TTA-UC-mediated prodrug activation process in TTA-CS.

Next, we tested the feasibility of prodrug activation using our TTA-CS system (Figure 2). The activation of the prodrug process was quantified by using the fluorescence measurement because the fluorescence at 498 nm of the coumarin moiety decreases when it is removed from the chlorambucil molecules (Figure S13). As shown in Figure S14, when we irradiated TTA-CS with a 650-nm light-emitting diode (LED) ( $100 \text{ mW cm}^{-2}$ ), the prodrug was uncaged, resulting in > 48% activation of the prodrug within 30 min, and a maximum photorelease of around 82% of the prodrug after 60 min. These results confirm that the prodrug can be activated by the TTA-upconversion process using far-red light. A similar nanocapsule consisting of the photosensitizers without the PEA emitter (termed BDP-F-CS) was designed as a non-emissive control. Excluding the possibility of the direct uncaging of chlorambucil by 650 nm light (Figure S15), upon 650 nm irradiation of BDP-F-CS for 60 min, no observable uncaged chlorambucil was detected. Moreover, the photorelease of chlorambucil was clearly dependent on the ON-OFF pattern of the LED excitation source (Figure 2). This result indicates that the release dose and duration can be precisely titrated by using far-red light under a low power density of  $100 \text{ mW cm}^{-2}$ .

To demonstrate the *in vitro* effectiveness of our system, cell viability experiments were conducted. Cancer cells (HeLa and 4T<sub>1</sub> cells) were incubated with TTA-CS for 12 h and then a low-power far-red LED was used. As shown in Figure S16, TTA-MSNs have insignificant toxicity with and without light. In addition, TTA-CS ( $0\text{--}375 \mu\text{g mL}^{-1}$ ) had negligible cell toxicity in the absence of LED light. However, upon irradiation with the far-red LED, TTA-CS presented significant toxicity towards both HeLa and 4T<sub>1</sub> cells. This result suggests that Cou-C is successfully photocleaved by TTA-UC and the hydrophilic anticancer drug chlorambucil is indeed released from TTA-CS into the cells, causing cancer cell death (Figure 3). The IC<sub>50</sub> under irradiation (half-maximal concentration of TTA-CS and Cou-C to cause cell death) was calculated to be  $235 \pm 5.9 \mu\text{g mL}^{-1}$  and  $2.74 \mu\text{g mL}^{-1}$  with HeLa cells, and  $320 \pm 6.3 \mu\text{g mL}^{-1}$  and  $3.64 \mu\text{g mL}^{-1}$  with 4T<sub>1</sub> cells, respectively.

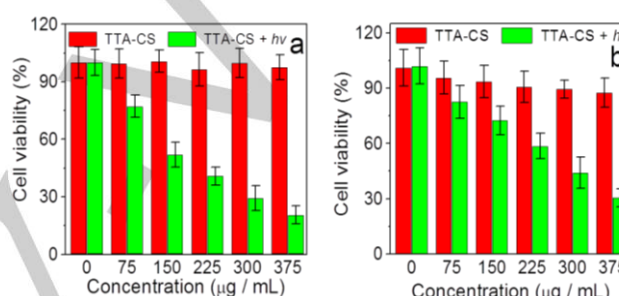


**Figure 3.** MTT assay of HeLa, 4T<sub>1</sub> cell viability with different concentrations of TTA-CS with and without light. a) HeLa cells; b) 4T<sub>1</sub> cells.  $\lambda_{\text{ex}} = 650 \text{ nm}$ , photon fluence ( $360 \text{ J cm}^{-2}$ ).

Prodrug photorelease mediated by far-red light was also evaluated by the calcein-AM/PI co-staining method.<sup>[13]</sup> In the absence of a far-red LED, we only observed bright green emission in the cancer cells, which suggests that TTA-CS itself did not kill cancer cells. However, in the presence of irradiation with a far-red LED, red fluorescence was observed in the cells, which suggests cell death. We did not observe significant cell death with prodrug-free core nanoparticles (TTA-MSNs) in the presence of LED irradiation (Figure S17). These results further demonstrated that far-red-light triggered TTA upconversion can activate prodrug photorelease and lead to cancer-cell-growth inhibition.

Since TTA-CS showed excellent cancer cell inhibition *in vitro*, we continued testing TTA-UC-induced prodrug release *in vivo*. First, we prepared 4T<sub>1</sub> tumor-bearing mice and divided them into four groups (Group 1: only PBS injection + irradiation; Group 2: TTA-CS injection but no irradiation; Group 3: TTA-MSNs and irradiation; Group 4: TTA-CS injection and irradiation). After 60 min of intratumor injection, tumor sites were then irradiated with a far red LED ( $100 \text{ mW cm}^{-2}$ ). The treatment outcome of TTA-CS to tumor was assessed by monitoring relative tumor volumes in mice, and tumor tissue ablation was also evaluated by H&E staining on tissue sections. As shown in Figure 4, no tumor-growth inhibition or tumor-tissue necrosis was observed in Group 1. Group 2 showed no tumor-growth inhibition or tumor-tissue necrosis, which indicates that TTA-CS itself cannot inhibit tumor growth. Group 3 also demonstrated insignificant cancer treatment efficiency, which suggests that the low-power red LED we used has low photothermal or other effects for cancer cell killing. In marked contrast, the tumor growth in Group 4 was

remarkably suppressed, and the tumor tissue showed obvious necrosis. These results indicate that the deep-blue upconversion-induced chlorambucil release from the prodrug (Cou-C) does lead to tumor-tissue ablation. To our knowledge, this is the first time that TTA-UC-induced photocleavage-based prodrug photorelease has been realized *in vivo* upon low-power irradiation with a far-red LED.

To determine the potential toxicity and side effects of TTA-CS, we measured the body-weight loss of the mice. As shown in **Figure S18**, mice treated with TTA-CS did not show apparent weight loss. Nine days after an intravenous injection of TTA-CS, the treated mice and untreated age-matched healthy mice were sacrificed, and the major organs including heart, liver, spleen, lung, and kidney were collected for H&E staining to evaluate the toxicity effects. No noticeable sign of organ damage was observed in the H&E-stained organ slices, which suggests that TTA-CS is safe for *in vivo* cancer treatment applications (**Figure S19**). A serum analysis was performed, as shown in **Table S2**; we observed no abnormal results from this analysis, which suggests that no observable inflammation was induced.

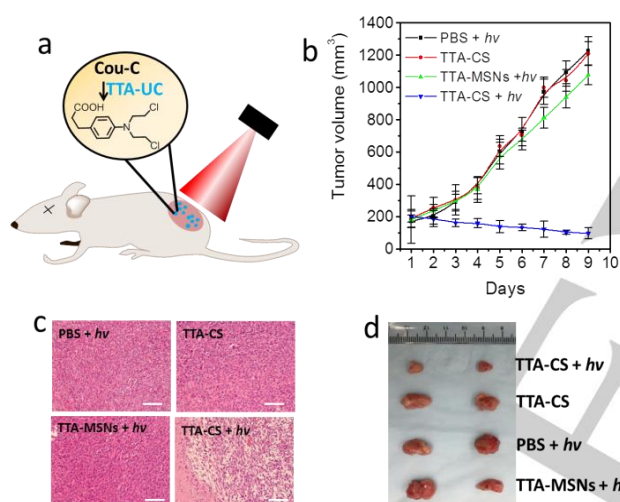


**Figure 4.** a) Illustration of the photocleavage drug release via TTA-UC. b) Tumor-growth inhibition by TTA-CS-mediated drug release in 4T<sub>1</sub> tumors; Values are means  $\pm$  s.e.m. ( $n = 5$  mice per group). c) H&E staining of tumor tissue sections from different treatment groups 9 days after treatment, scale bar represents 50  $\mu\text{m}$ . d) Representative digital photos of tumors for the four groups of mice. Photon flux ( $180 \text{ J cm}^{-2}$ ).

In conclusion, we designed the longest known anti-Stokes shift TTA-UC system. This new TTA system has robust brightness from the far-red to deep-blue regions. Thanks to these properties, we were able to develop a TTA core-shell-structured drug-delivery capsule that can effectively activate anticancer prodrug release *in vitro* and *in vivo* with a biocompatible far-red LED light. This new organic TTA upconversion system not only offers a new nanoplatform for spatiotemporally controlled cancer therapy, but also has great potential for numerous photonic and biophotonic applications.

## Acknowledgements

This research was supported by the National Institutes of Health R01MH103133 the Human Frontier Science RGY-0090/2014, and UMass OTCV award.

**Keywords:** Triplet–triplet annihilation upconversion • Anti-Stokes shifts • BODIPY • Prodrug activation • Anticancer

- [1] a) C. Brieke, F. Rohrbach, A. Gottschalk, G. Mayer, A. Heckel, *Angew. Chem.* **2012**, *124*, 8572–8604; *Angew. Chem. Int. Ed.* **2012**, *51*, 8446–8476; b) G. Bort, T. Gallavardin, D. Ogden, P. I. Dalko, *Angew. Chem.* **2013**, *125*, 4622–4634; *Angew. Chem. Int. Ed.* **2013**, *52*, 4526–4537; c) N. C. Fan, F. Y. Cheng, J. A. A. Ho, C. S. Yeh, *Angew. Chem.* **2012**, *124*, 8936–8940; *Angew. Chem. Int. Ed.* **2012**, *51*, 8806–8810; d) S. Li, B. A. Moosa, J. G. Croissant, N. M. Khashab, *Angew. Chem.* **2015**, *127*, 6908–6912; *Angew. Chem. Int. Ed.* **2015**, *54*, 6804–6808; e) J. Lu, E. Choi, F. Tamanoi, J. I. Zink, *Small* **2008**, *4*, 421–426; f) Q. Yuan, Y. F. Zhang, T. Chen, D. Q. Lu, Z. L. Zhao, X. B. Zhang, Z. X. Li, C. H. Yan, W. H. Tan, *ACS Nano* **2012**, *6*, 6337–6344.
- [2] a) J. Croissant, M. Maynadier, A. Gallud, H. P. N'Dongo, J. L. Nyalosaso, G. Derrien, C. Charnay, J. O. Durand, L. Raehm, F. Serein-Spirau, N. Cheminet, T. Jarrosson, O. Mongin, M. Blanchard-Desce, M. Gary-Bobo, M. Garcia, J. Lu, F. Tamanoi, D. Tarn, T. M. Guardado-Alvarez, J. I. Zink, *Angew. Chem.* **2013**, *125*, 14058–14062; *Angew. Chem. Int. Ed.* **2013**, *52*, 13813–13817; b) L. Fenno, O. Yizhar, K. Deisseroth, *Ann. Rev. Neurosci.* **2011**, *34*, 389–412; c) N. Huebsch, C. J. Kearney, X. H. Zhao, J. Kim, C. A. Cezar, Z. G. Suo, D. J. Mooney, *Proc. Natl. Acad. Sci. USA* **2014**, *111*, 9762–9767; d) N. S. Satarkar, J. Z. Hilt, *J. Control. Release* **2008**, *130*, 246–251.
- [3] a) G. Y. Chen, J. Shen, T. Y. Ohulchanskyy, N. J. Patel, A. Kutikov, Z. P. Li, J. Song, R. K. Pandey, H. Agren, P. N. Prasad, G. Han, *ACS Nano* **2012**, *6*, 8280–8287; b) X. Wu, G. Y. Chen, J. Shen, Z. J. Li, Y. W. Zhang, G. Han, *Bioconjugate. Chem.* **2015**, *26*, 166–175; c) D. M. Yang, P. A. Ma, Z. Y. Hou, Z. Y. Cheng, C. X. Li, J. Lin, *Chem. Soc. Rev.* **2015**, *44*, 1416–1448; d) W. Zheng, P. Huang, D. T. Tu, E. Ma, H. M. Zhu, X. Y. Chen, *Chem. Soc. Rev.* **2015**, *44*, 1379–1415.
- [4] a) P. P. Goswami, A. Syed, C. L. Beck, T. R. Albright, K. M. Mahoney, R. Unash, E. A. Smith, A. H. Winter, *J. Am. Chem. Soc.* **2015**, *137*, 3783–3786; b) A. Jana, K. T. Nguyen, X. Li, P. C. Zhu, N. S. Tan, H. Agren, Y. L. Zhao, *ACS Nano* **2014**, *8*, 5939–5952; c) P. Klan, T. Solomek, C. G. Bochet, A. Blanc, R. Givens, M. Rubina, V. Popik, A. Kostikov, J. Wirz, *Chem. Rev.* **2013**, *113*, 119–191; d) G. Liu, W. Liu, C. M. Dong, *Polym. Chem.* **2013**, *4*, 3431–3443; e) J. P. Pellois, T. W. Muir, *Angew. Chem.* **2005**, *117*, 5859–5863; *Angew. Chem. Int. Ed.* **2005**, *44*, 5713–5717; f) S. R. Trenor, A. R. Shultz, B. J. Love, T. E. Long, *Chem. Rev.* **2004**, *104*, 3059–3077.
- [5] G. Jalani, R. Naccache, D. H. Rosenzweig, L. Haglund, F. Vetrone, M. Cerruti, *J. Am. Chem. Soc.* **2016**, *138*, 1078–1083.
- [6] a) A. Gnach, T. Lipinski, A. Bednarkiewicz, J. Rybka, J. A. Capobianco, *Chem. Soc. Rev.* **2015**, *44*, 1561–1584; b) Y. Sun, W. Feng, P. Y. Yang, C. H. Huang, F. Y. Li, *Chem. Soc. Rev.* **2015**, *44*, 1509–1525.
- [7] a) T. N. Singh-Rachford, F. N. Castellano, *Coord. Chem. Rev.* **2010**, *254*, 2560–2573; b) J. Z. Zhao, S. M. Ji, H. M. Guo, *RSC Adv.* **2011**, *1*, 937–950; c) J. Z. Zhao, W. H. Wu, J. F. Sun, S. Guo, *Chem. Soc. Rev.* **2013**, *42*, 5323–5351; d) J. Z. Zhao, K. J. Xu, W. B. Yang, Z. J. Wang, F. F. Zhong, *Chem. Soc. Rev.* **2015**, *44*, 8904–8939; e) J. Zhou, Q. Liu, W. Feng, Y. Sun, F. Y. Li, *Chem. Rev.* **2015**, *115*, 395–465. f) A. J. Svagan, D. Busko, Y. Avlasevich, G. Glasser, S. Balushev, K. Landfester, *ACS Nano* **2014**, *8*, 8198–8207; g) J.-H. Kim, J.-H. Kim, *ACS Photonics*, **2015**, *2*, 633–638; h) P. Ceroni, *Chem. Eur. J.* **2011**, *17*, 9560–9564; i) N. Yanai, N. Kimizuka, *Chem. Commun.* **2016**, *52*, 5354–5370; j) S. M. Borisov, C. Larndorfer, I. Klimant, *Adv. Funct. Mater.* **2012**, *22*, 4360–4368.
- [8] W. P. Wang, Q. Liu, C. Y. Zhan, A. Barhoumi, T. S. Yang, R. G. Wylie, P. A. Armstrong, D. S. Kohane, *Nano Lett.* **2015**, *15*, 6332–6338.

- [9] a) L. He, Y. W. Zhang, G. L. Ma, P. Tan, Z. J. Li, S. B. Zang, X. Wu, J. Jing, S. H. Fang, L. J. Zhou, Y. J. Wang, Y. Huang, P. G. Hogan, G. Han, Y. B. Zhou, *elife* **2015**, *4*; b) Q. N. Lin, Q. Huang, C. Y. Li, C. Y. Bao, Z. Z. Liu, F. Y. Li, L. Y. Zhu, *J. Am. Chem. Soc.* **2010**, *132*, 10645–10647; c) O. Seok, K. Hyun, S. Song, J. Conde, H-i. Kim, N. Artzi, J-H. Kim. *ACS Nano*, **2016**, *10*, 1512–1521.
- [10] a) S. H. C. Askes, A. Bahreman, S. Bonnet, *Angew. Chem.* **2014**, *126*, 1047–1051; *Angew. Chem. Int. Ed.* **2014**, *53*, 1029–1033; b) T. N. Singh-Rachford, A. Haefele, R. Ziessel, F. N. Castellano. *J. Am. Chem. Soc.*, **2008**, *130*, 16164–16165; c) Q. Liu, B. Yin, T. Yang, Y. Yang, Z. Shen, P. Yao, F. Li. *J. Am. Chem. Soc.* **2013**, *135*, 5029–5037.
- [11] a) Y. Murakami, Y. Himuro, T. Ito, R. Morita, K. Niimi, N. Kiyoyanagi, *J. Phys. Chem. B*, **2016**, *120*, 748–755. b) A. Monguzzi, J. Mezyk, F. Scotognella, R. Tubino, F. Meinardi, *Phys. Rev. B* **2008**, *78*, 195112.
- [12] L. Z. Zhao, J. J. Peng, Q. Huang, C. Y. Li, M. Chen, Y. Sun, Q. N. Lin, L. Y. Zhu, F. Y. Li, *Adv. Funct. Mater.* **2014**, *24*, 363–371.
- [13] Y. Li, J. Tang, D.-X. Pan, L.-D. Sun, C. Chen, Y. Liu, Y.-F. Wang, S. Shi, C.-H. Yan, *ACS Nano*, **2016**, *10*, 2766–2773.

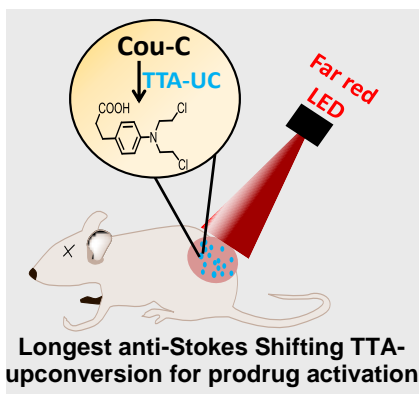
Entry for the Table of Contents (Please choose one layout)

Layout 1:

## COMMUNICATION

**Far Red light means go for organic upconversion prodrug activation:**

A strategy is presented for a new triplet-triplet annihilation upconversion that has robust brightness and the record longest anti-Stokes shift from far red to deep blue. TTA core-shell-structured prodrug photorelease nanocapsules are developed that operate with a low-power density far-red-LED light and show effective prodrug activation control ability and potent tumor-growth inhibition in vivo.



Ling Huang, Yang Zhao, He Zhang, Kai Huang, Jinyi Yang, and Gang Han

Page No. – Page No.

Expanding Anti-Stokes Shifting in Triplet–Triplet Annihilation Upconversion for In Vivo Anticancer Prodrug Activation